cross-correlating the corresponding syllables, as follows. Introductory syllables were excluded because for the RA they are not associated with a precise temporal pattern of activity (Fig. 2A). Motif syllables comprising simple harmonic stacks were also excluded because they lack meaningful time-varying frequency modulation, which resulted in unreliable cross-correlations. This left acoustically complex syllables of motifs for analysis. The acoustic records were scored without reference to the associated spike trains to eliminate recordings with acoustic clutter (background cage noises, calls of females). Six additional syllables were eliminated on this basis because less than 10 acoustically uncontaminated exemplars were identified, preventing meaningful statistical analysis. For each of the 15 resultant syllable types (15 neurons, three birds), a "referent" syllable was chosen by manual inspection of spectrographs of the set of exemplar syllables. The spectrograph of each exemplar syllable was then cross-correlated with the spectrograph of the referent [C. W. Clark, P. Marler, P. Beeman, *Ethology* **76**, 101 (1987)]. We then adjusted the temporal registry of each spike train associated with each exemplar syllable, relative to the spike train associated with the referent syllable, by applying a shift in time (translation) based on the position of the peak in the correlation function. The time shifts were typically quite small (τ = 3.00 ± 2.31 ms, n = 1436 cross-correlations of referent and exemplar syllables), implying that the original manual segmentation was quite accurate; nevertheless, this shift significantly affected the temporal registry of spike trains.

10. An optimal translation of the spike trains was applied on a burst-by-burst basis to minimize the global difference in spike timing. That is, this procedure aligned each spike burst independent of the acoustics of associated notes. The acoustic procedure of (*9*) failed to further improve the temporal registry of spike bursts when applied on a note-by-note basis. This failure may be the result of the fine temporal resolution of RA neuronal discharge patterns overwhelming inherent limitations in time-frequency resolution in the calculation of spectrographs based on short-time Fourier transformations [G. D. Bergland, *IEEE Spectrum* **7**, 41 (1969)]. Nevertheless, it implies that we were not able to quantitatively demonstrate that the timing of each burst pattern was associated with the timing of each note. The RA exhibits a myotopic organization [D. S. Vicario, *J. Neurobiol.* **22**, 63 (1991)], hence the activity of RA neurons may be associated with activation of individual muscles or groups of muscles.
11. S. Nowicki and R. R. Capranica, *Science* **231**, 1297 (1986); F. Goller and R. A. Suthers, *Nature* **373**, 63 (1995); M. W. Westneat, J. H. J. Long, W. Hoese, S. Nowicki, *J. Exp. Biol.* **182**, 147 (1993).
12. E. E. Fetz, in *Movement Control*, P. Cordo and S. Harnad, Eds. (Cambridge Univ. Press, Cambridge, 1994), pp. 77–88.
13. H. Williams and D. Vicario, *J. Neurobiol.* **24**, 903 (1993).
14. See also E. T. Vu, M. E. Mazurek, Y.-C. Kuo, *J. Neurosci.* **14**, 6924 (1994).
15. N. Tinbergen, *Symp. Soc. Exp. Biol.* **4**, 305 (1950); *The Study of Instinct* (Oxford Univ. Press, Oxford, 1951).
16. R. Mooney, *J. Neurosci.* **12**, 2464 (1992).
17. M. Abeles *et al.*, *Proc. Natl. Acad. Sci. U.S.A.* **92**, 8616 (1995); E. Vaadia *et al.*, *Nature* **373**, 515 (1995).
18. R. Llinás, *Cold Spring Harbor Symp. Quant. Biol.* **55**, 933 (1990).
19. C. E. Carr, W. Heiligenberg, G. J. Rose, *J. Neurosci.* **6**, 107 (1986); C. E. Carr and M. Konishi, *Proc. Natl. Acad. Sci. U.S.A.* **85**, 8311 (1988); E. Ahissar *et al.*, *Science* **257**, 1412 (1992); G. H. Recanzone, M. M. Merzenich, C. E. Schreiner, *J. Neurophysiol.* **67**, 1071 (1992); J. C. Middlebrooks, A. E. Clock, L. Xu, D. M. Green, *Science* **264**, 842 (1994); R. C. de Charms and M. M. Merzenich, *Nature* **381**, 610 (1996); W. Bair and C. Koch, *Neural Comp.* **8**, 1184 (1996).
20. To construct an eMAH, we defined a canonical song: the most common number of introductory syllables, the most common sequence of syllables within a motif, and the most common number of motifs. The eMAH was derived from concatenation of individual MAHs corresponding to each syllable type within its specific context of the canonical song—for example, all spikes corresponding to syllable E in the first motif or all spikes corresponding to syllable E in the second motif (Fig. 1B). Individual MAHs were calculated starting 50 ms before their corresponding syllable.
21. J. J. Gilpin manufactured the devices for chronic recording. A. S. Dave collected the data for one of the HVc birds. We thank A. S. Dave, S. E. Anderson, and J. A. Kogan, who provided valuable advice and assistance on aspects of the data analysis. M. Konishi and P. S. Ulinski provided useful critiques of the manuscript. Supported by a grant from the Whitehall Foundation (M91-05). A.C.Y. was supported by an NIH predoctoral fellowship (1 F31 MH10151).

26 April 1996; accepted 8 August 1996

Conformational States of the Nuclear Pore Complex Induced by Depletion of Nuclear Ca^{2+} Stores

Carmen Perez-Terzic, Jason Pyle, Marisa Jaconi, Lisa Stehno-Bittel,* David E. Clapham†

The nuclear pore complex (NPC) is essential for the transit of molecules between the cytoplasm and nucleoplasm of a cell and until recently was thought to allow intermediate-sized molecules (relative molecular mass of ~10,000) to diffuse freely across the nuclear envelope. However, the depletion of calcium from the nuclear envelope of *Xenopus laevis* oocytes was shown to regulate the passage of intermediate-sized molecules. Two distinct conformational states of the NPC were observed by field emission scanning electron microscopy and atomic force microscopy. A central plug occluded the NPC channel after nuclear calcium stores had been depleted and free diffusion of intermediate-sized molecules had been blocked. Thus, the NPC conformation appears to gate molecular movement across the nuclear envelope.

The NPC spans the nuclear envelope and mediates the selective exchange of proteins, mRNA, and ions between the cytoplasm and the nucleus (*1*). The NPC is a tripartite cylindrical structure surrounded by an octagonal spoked ring complex (*2–4*). Conformational changes within the NPC and its transporter (which we call the central plug) are thought to regulate movement across the nuclear envelope (*3–5*). Depletion of the nuclear calcium (Ca^{2+}) stores inhibits diffusion through the NPC of molecules with a relative molecular mass (M_r) of ~10,000 that lack nuclear localization sequences (*6–8*). To directly assess whether depletion of Ca^{2+} from nuclear stores triggers a change in the structure of NPC, we used field emission scanning electron microscopy (FESEM) and atomic force microscopy (AFM) to image the NPC central pore. We found that depletion of nuclear cisternal Ca^{2+}, as measured by laser scanning confocal microscopy (*7*), blocked transport of intermediate-sized molecules and that this block was associated with the appearance of an NPC central plug.

Department of Pharmacology, Mayo Foundation, Rochester, MN 55905, USA.

*Present address: University of Kansas Medical Center, 3901 Rainbow Boulevard, Kansas City, KS 66160–7601, USA.

†To whom correspondence should be addressed. E-mail: clapham@mayo.edu

Nuclear envelopes isolated from *X. laevis* oocytes were imaged by FESEM (*9*). In nuclei isolated in Ca^{2+}-containing solutions (~200 nM), the majority of NPCs displayed typical eightfold symmetry (*2–4*), but most lacked the central plug (Fig. 1A). The absence of the central plug in NPCs has been attributed to specimen preparation (*3, 4, 10, 11*). After we first treated nuclei with the physiologically important second messenger, inositol 1,4,5-trisphosphate [$Ins(1,4,5)P_3$; 1 μM for 10 min] to open Ca^{2+} channels in the nuclear envelope and to deplete Ca^{2+} from nuclear stores (*12, 13*), we found that the majority of NPCs contained the central plug (Fig. 1B). NPCs from nuclei incubated in Ca^{2+}-containing solution had occupancy of their central pores of 6.9 ± 0.5% (mean ± SD; n = 14 nuclei, 826 NPCs) compared with 91.9 ± 1.2% (n = 10 nuclei; 630 NPCs) for NPCs of nuclei treated with $Ins(1,4,5)P_3$ in the same solution. Treatment of nuclei with other inositol phosphates, which have a low affinity for the $InsP_3$ receptor and did not release Ca^{2+} from the nuclear store at 1 μM concentrations (*12, 14*), failed to induce the appearance of the central plug in NPCs of isolated nuclear envelopes. In nuclei treated with inositol 1,3,4-trisphosphate [$Ins(1,3,4)P_3$; 1 μM; n = 8 nuclei; 488 NPCs] or inositol 1,3,4,5-tetrakisphosphate [1 μM $Ins(1,3,4,5)P_4$; n = 9 nuclei, 684

NPCs], the average percentage of NPC occupancy by the plug was 9.1 ± 1.1% and 7.3 ± 0.8%, respectively. Conversely, after nuclei were incubated in low-Ca^{2+} medium (10 nM for 20 min) to deplete nuclear Ca^{2+} stores, 86.6 ± 3.5% (n = 5 nuclei, 320 NPCs) of NPCs contained the central plug. Depletion of Ca^{2+} stores by incubation in the membrane-permeant form of the Ca^{2+} chelator 10 mM BAPTA-AM [bis(2-aminophenoxy)ethane-*N*,*N*,*N*′,*N*′-tetracetic acid; n = 4 nuclei, 352 NPCs] was also associated with the appearance of the central plug in 89.5 ± 4.7% of the total number of NPCs observed. To test the reversibility of the process, we incubated nuclei in the presence of $Ins(1,4,5)P_3$ (1 μM for 10 min) to deplete the nuclear Ca^{2+} stores. The same nuclei were then incubated in a solution containing adenosine triphosphate (ATP; 1 mM) and Ca^{2+} (2 μM for 10 min), conditions that replenish the nuclear Ca^{2+} store (*7*, *13*). Under these conditions, only 4.8 ± 0.7% (n = 5 nuclei, 470 NPCs) of the NPCs contained the central plug. Thus, depletion of nuclear Ca^{2+} stores by any one of several methods that block free diffusion of ~10,000 M_r molecules (*6*, *7*) also resulted in NPC pore occlusion by the central plug (Fig. 1C).

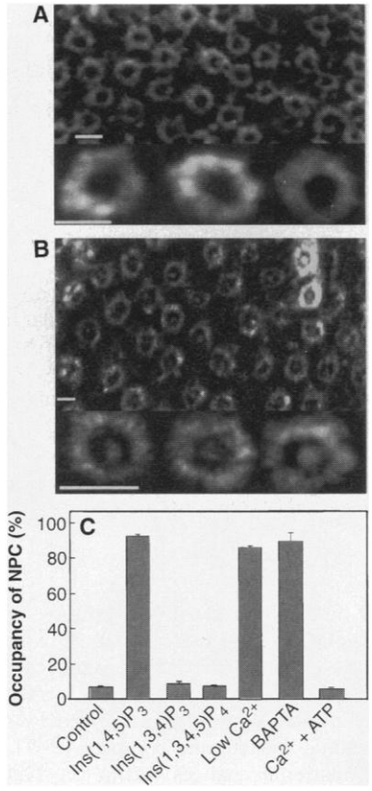

Fig. 1. FESEM images of nuclear envelopes from *Xenopus* oocytes. (**A**) Representative area of a nuclear envelope preincubated in 100 nM Ca^{2+}-containing solution. Individual NPCs displayed eightfold symmetry around an apparently empty central pore. (Inset) Three NPCs presented at a higher magnification. Bars, 100 nm. (**B**) Representative area of a fixed nuclear envelope isolated from a nucleus incubated for 10 min in 1 μM $Ins(1,4,5)P_3$. Individual NPCs displayed eightfold symmetry around a filled central pore. (Inset) Three NPCs presented at a higher magnification all contain the central plug. Radial arms appear faintly at the periphery of the central plug. Bars, 100 nm. (**C**) Percent occupancy of the NPC channel correlates with nuclear Ca^{2+} store depletion. The central plug was present in 6.9 ± 5% (n = 14) of control NPCs (nuclei incubated in Ca^{2+}-containing solution) but increased after treatment of nuclei with agents that depleted the nuclear Ca^{2+} stores [$Ins(1,4,5)P_3$, n = 10 nuclei; BAPTA-AM, n = 4 nuclei; and EGTA-Ca^{2+} solutions (10 nM), n = 5 nuclei]. Compounds that did not release Ca^{2+} from nuclear stores at 1 μM concentrations [$Ins(1,3,4)P_3$, (n = 8 nuclei) and $Ins(1,3,4,5)P_4$, (n = 9 nuclei)] did not increase the occupancy of the NPC central pore. After depletion of the nuclear Ca^{2+} store by incubation in 1 μM $InsP_3$, the store was replenished with 1 mM ATP + 2 μM Ca^{2+}. These replenished preparations again exhibited few nuclear plug–containing NPCs, which demonstrated that the blocking process was reversible (n = 5 nuclei).

We used AFM to obtain surface images of a fixed nuclear envelope isolated in Ca^{2+}-containing solution (*15*). At this resolution, the eightfold symmetry of individual NPCs was apparent. The central plug was ~10 nm below the cytoplasmic ring of the NPC (89 ± 2% of NPCs; n = 5 nuclei, 45 NPCs) (Fig. 2A). In nuclei first incubated in 1 μM $Ins(1,4,5)P_3$, AFM revealed a plug level with the outer rim of the NPC in 36 of 38 NPCs imaged (95 ± 2%; n = 5 nuclei). The material occluding the pore constitutes the central plug, which has been vertically displaced toward the cytoplasmic surface of the NPC after depletion of the nuclear Ca^{2+} store (Fig. 2C). The AFM profile of individual NPCs from nuclear envelopes in Ca^{2+}-containing solution shows a depression (the central pore) circumscribed by two raised areas (the sides of the NPC) (Fig. 2B). In nuclei treated with $Ins(1,4,5)P_3$, the central pore was filled (Fig. 2D). The apparent depth of the central depression averaged 11.6 ± 0.8 nm (n = 8 profiles) in nuclei incubated in

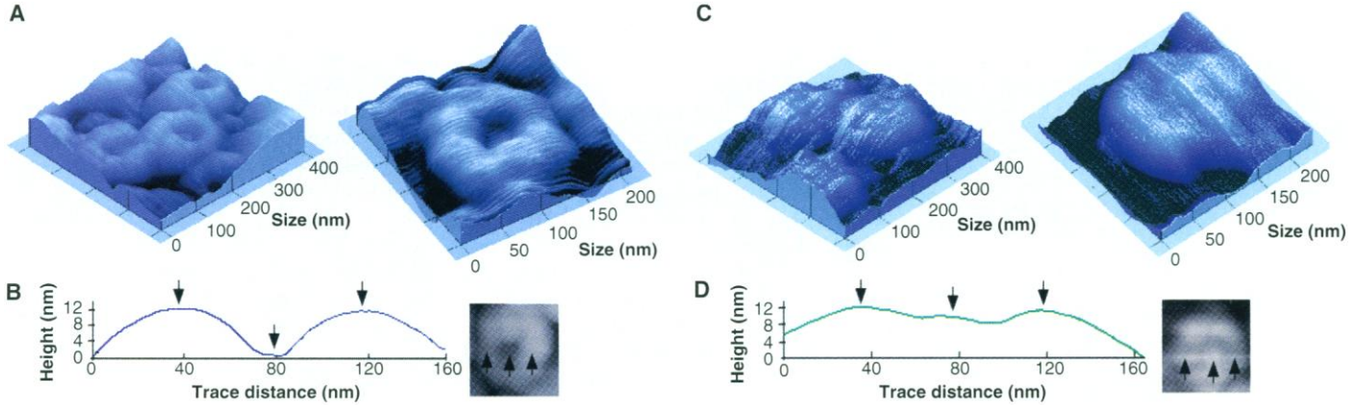

Fig. 2. Atomic force topographic images from fixed *Xenopus* oocyte nuclear envelopes. (**A**) Three-dimensional images of NPCs from nuclei incubated in Ca^{2+}-containing solutions. The octagonal structures of the individual NPCs have a clearly defined central pore. The plug is positioned ~10 nm below the cytoplasmic ring of the central pore. Outer NPC diameter is 156 nm. (**B**) NPC height profile obtained from a nucleus incubated in Ca^{2+}-containing (200 nM) solution. Note the central depression ~10 nm below the cytoplasmic surface of the NPC. Measurements were not limited by the z axis resolution of the instrument because, depending on the conditions and tips, the z range is up to 1 μm. Arrows indicating positions in the graph correspond to positions indicated by arrows on the structure in the inset. (**C**) Three-dimensional images of NPCs from nuclei treated with $Ins(1,4,5)P_3$ (1 μM). Individual NPCs are occluded. Outer NPC diameter is 163 nm. (**D**) NPC height profile obtained from a nucleus incubated for 10 min in $Ins(1,4,5)P_3$ (1 μM). The diminished central depression is now only ~2 nm below the cytoplasmic surface of the NPC. Arrows in the graph correspond to positions indicated by arrows on the structure in the inset.

Ca^{2+}-containing solutions and 2.1 ± 0.2 nm (n = 10 profiles) in NPCs from nuclei incubated in Ins(1,4,5)P_3. Thus, results obtained by AFM support the conclusions made on the basis of FESEM and transmission electron microscopy (TEM) measurements despite different sample preparation procedures and dissimilar physical methods used to probe the sample.

The external diameter of the cytosolic ring measured by AFM was 149.1 ± 5.1 nm (n = 11) for nuclear envelopes isolated in Ca^{2+}-containing solutions. The diameter changed only slightly after treatment with 1 μM Ins(1,4,5)P_3 (162.5 ± 4.3 nm; n = 11). However, the inner diameter of the NPC channel measured 67.9 ± 2.3 nm (n = 12) for nuclear envelopes isolated in Ca^{2+}-containing solutions but decreased to 34.2 ± 1.8 nm (n = 12) after treatment with 1 μM Ins(1,4,5)P_3. This conformational change is consistent with Akey's model of the NPC in which the pore structure closes in, much like a camera iris (3). We speculate that depletion of the nuclear Ca^{2+} store resulted in the transporter plug being moved into its blocking position in the now narrowed pore, occluding most of the NPC channel, a process analogous to the movement of a caged ball valve. We hypothesize that this conformational switch blocks the entry or exit by passive diffusion of all but small molecules (ions and molecules ≤500 M_r) (7).

This study of the nucleus has been limited to freely diffusing molecules; we have not determined whether the central (transporter) plug can admit larger molecules containing nuclear localization sequences into the cell after Ca^{2+} store depletion. Depletion of Ca^{2+} stores in living (intact) cells also inhibits signal-mediated transport into the nucleus (6). Several mechanisms could trigger a specific conformational change of the NPC when the Ca^{2+} store is depleted. For example, the integral NPC transmembrane glycoprotein gp210 contains an EF-hand (helix-loop-helix) Ca^{2+}-binding domain in the nuclear cisterna (8) and is a logical candidate for such a mechanism. The NPC is thus likely to be a dynamic structure sensitive to nuclear cisternal Ca^{2+} concentration that controls free diffusion of intermediate-sized molecules across the nuclear membranes. The major challenge will be to determine the purpose and context of this gating mechanism.

REFERENCES AND NOTES

1. J. A. Hanover, *FASEB J.* **6**, 2288 (1992); M. W. Goldberg and T. D. Allen, *Curr. Opin. Cell Biol.* **7**, 301 (1995); D. Gorlich and I. W. Mattaj, *Science* **271**, 1513 (1996).
2. P. N. T. Unwin and R. A. Milligan, *J. Cell Biol.* **93**, 63 (1982).
3. C. W. Akey, *Biophys. J.* **58**, 341 (1990).
4. _____ and M. R. Radermacher, *J. Cell. Biol.* **122**, 1 (1993).
5. C. W. Akey, *ibid.* **109**, 955 (1989); *J. Mol. Biol.* **248**, 273 (1995).
6. U. F. Greber and L. Gerace, *J. Cell Biol.* **128**, 5 (1995).
7. L. Stehno-Bittel, C. Perez-Terzic, D. E. Clapham, *Science* **270**, 1835 (1995).
8. U. F. Greber, A. Senior, L. Gerace, *EMBO J.* **9**, 1495 (1990); U. F. Greber and L. Gerace, *J. Cell Biol.* **116**, 15 (1992).
9. Mature oocytes were surgically removed from adult *X. laevis* females as described [J. D. Lechleiter and D. E. Clapham, *Cell* **69**, 283 (1992)]. Oocytes were enucleated manually by dissecting the oocyte along its equator. Nuclei were removed and transferred to low-salt buffer (LSB) [1 mM triethanolamine–HCl, 0.5 mM $MgCl_2$ (pH 7.5)] to remove adhering cytoplasm (J. E. Hinshaw, B. O. Carragher, R. A. Milligan, *ibid.*, p. 1133). Isolated nuclei were then incubated for 10 min in mock intracellular solution [140 mM KCl, 10 mM Hepes, and 3 mM $MgCl_2$ (pH 7.2)] containing in some experiments either Ins(1,4,5)P_3, Ins(1,3,4)P_3, Ins(1,3,4,5)P_4, ~10 nM free Ca^{2+} with 10 mM EGTA [E. Neher, *J. Physiol. (London)* **395**, 193 (1988)], 10 mM BAPTA-AM, or 1 mM ATP with 2 μM Ca^{2+}. Because thapsigargin does not deplete the nuclear Ca^{2+} store as it does the endoplasmic reticulum store, we were unable to use it as a pharmacological tool. The nuclei were then fixed for 4 hours in a buffer solution containing 1% glutaraldehyde and 4% formaldehyde (pH 7.2). The nuclear envelope was spread manually on an electron microscope carbon grid and prepared for critical-point drying. The specimen was rinsed twice in 0.1 M phosphate buffer (pH 7.2) and in buffer supplemented with 1% osmium for 10 min. Samples were dehydrated with incremental concentrations of ethanol before being dried in a critical-point dryer (Ted Pella, Inc., Tustin, CA). Fixed critical point–dried intact nuclei and nuclear envelopes directly adhered to double-sided carbon tape on brass mounts and were coated with a discontinuous layer of platinum (~1 nm thick) by use of an Ion Tech indirect argon ion–beam sputtering system (VCR Group, San Francisco, CA) operating at an accelerating voltage of 9.5 kV and 4.2 mA. Samples were examined at various accelerating voltages (1.0, 2.4, 3.5, and 5.0 kV) in a Hitachi S-900 FESEM in the secondary electron mode, and images were recorded on Polaroid Type 52 or Type 55 film. Results were expressed as means ± SEM. Transmission electron microscopy of NPCs gave similar results (data not shown). All experiments were performed at room temperature (22° ± 2°C).
10. N. Pante and U. Aebi, *J. Cell Biol.* **122**, 977 (1993).
11. M. Jarnik and U. Aebi, *J. Struct. Biol.* **107**, 291 (1991).
12. L. Stehno-Bittel, A. Luckhoff, D. E. Clapham, *Neuron* **14**, 163 (1995).
13. P. Nicotera, B. Zhivotovsky, S. Orrenius, *Cell Calcium* **16**, 279 (1994).
14. D. O. Mak and J. K. Foskett, *J. Biol. Chem.* **269**, 29375 (1994).
15. AFM uses deflection of a fine probe to gauge the force, and hence physical boundary, of structures. The resolution of AFM is limited primarily by probe tip size and shape, but it is generally possible to resolve nanometer structures on biological surfaces. Repetitive scanning of the probe across the surface to be imaged defines a three-dimensional topographic map [G. Binnig, C. F. Quate, C. Gerber, *Phys. Rev. Lett.* **129**, 930 (1986); M. Radmacher, R. W. Tillmann, M. Fritz, H. E. Gaub, *Science* **257**, 1900 (1992)]. The nuclear envelope was prepared and fixed as described for FESEM except that after fixation, the nuclear envelope was spread on a clean coverslip glass and air-dried before sampling. All AFM images were obtained with AutoProbe LS (Park, Scientific Instruments, Sunnyvale, CA) modified for biological samples, and analyzed by ProScan software, version 1.1 (Park, Scientific Instruments). Both pyramidal silicon nitride and sharpened silicon nitride tips with chrome coating were used (spring constant, 0.08 N/m). Images were obtained with an average scanning speed of 3 Hz. Sample scanning was performed in constant-force mode with probe sample force maintained ≤1 nN. Results were expressed as means ± SEM. Experiments were performed at 22° ± 2°C.

16. Supported by an NIH grant to D.E.C. We thank D. Braddock and V. Parpura for technical assistance with the AFM, C. Frethem (University of Minnesota) for the use of the FESEM, J. Charlesworth (Mayo Foundation) for use of the critical-point dryer, and J. Chong and A. Terzic for helpful comments on the manuscript.

17 May 1996; accepted 18 July 1996

Discover a new sequence.

Visit the SCIENCE On-line Web site and you just may find the key piece of information you need for your research. The fully searchable database of research abstracts and news summaries allows you to look through current and back issues of SCIENCE on the World Wide Web. Tap into the sequence below and see SCIENCE On-line for yourself.

NEW URL **http://www.sciencemag.org**

SCIENCE